

# THE CONTROL SYSTEM OF THE FOUR-BOUNCE CRYSTAL MONOCHROMATORS FOR SIRIUS/LNLS BEAMLINES

L. Martins dos Santos\*, J. H. Rezende, M. Saveri Silva, H. C. N. Tolentino,  
L. M. Kofukuda, G. N. Kontogiorgos, P.D. Aranha, M. A. L. Moraes,  
Brazilian Synchrotron Light Laboratory (LNLS), Campinas, Brazil

## Abstract

CARNAÚBA (Coherent X-ray Nanoprobe) and CATERETÊ (Coherent and Time-Resolved Scattering) are the longest beamlines in Sirius – the 4th generation light source at the Brazilian Synchrotron Light Laboratory (LNLS). They comprise Four-Bounce Crystal Monochromators (4CM) for energy selection with strict stability and performance requirements. The motion control architecture implemented for this class of instruments was based on Omron Delta Tau Power Brick LV, controller with PWM amplifier. The 4CM was in-house designed and consists of two channel-cut silicon crystals whose angular position is given by two direct-drive actuators. A linear actuator mounted between the crystals moves a diagnostic device and a mask used to obstruct spurious diffractions and reflections. The system is assembled in an ultra-high vacuum (UHV) chamber onto a motorized granite bench that permits the alignment and the operation with pink-beam. This work details the motion control approach for axes coordination and depicts how the implemented methods led to the achievement of the desired stability, considering the impact of current control, in addition to benchmarking with manufacturer solution.

## INTRODUCTION

The Four-Bounce Crystal Monochromators (4CM) was in-house designed to compose the set of optical systems in the longest beamlines in Sirius [1]: CARNAÚBA [2] (Coherent X-ray Nanoprobe) and CATERETÊ [3] (Coherent and Time-Resolved Scattering).

The energy is selected by two channel-cut silicon crystals whose angular position is given by two direct-drive actuators. A mask, mounted between the crystals, is used to obstruct spurious diffractions, having as actuator a linear stage.

The system is assembled in an ultra-high vacuum (UHV) chamber onto a motorized granite bench that permits the alignment and the operation with pink-beam.

The adopted motion controller for this system was the Omron Delta Tau Power Brick LV (PBLV) and his PWM amplifier. This works discuss the methods that led to achieve the requirements of stability and coordination, considering current control influence, and compares with manufacturer control solution, Aerotech Ensemble Epaq MR (Epaq).

\* leandro.martins@lnls.br

## SYSTEM ARCHITECTURE

### Granite Bench

The granite bench is designed to both ensure high stiffness and allow the movement for alignment [4] of the monochromator and operation with pink beam, moving the UHV chamber to a position that the beam passes between the crystals.

Air-bearings in the bottom and top granite interface permits a frictionless motion in the translation in the X direction and rotation in the Y direction.

Furthermore, three levelers that supports the bottom granite compounds the translation in Y direction and rotations in X and Z directions.

The actuators of the granite bench are 2-phase stepper motors. The feedback of the position are made with a Heidenhain's quadrature incremental length-gauge for each leveler and a pair Renishaw's BiSS-C absolute linear encoder.

Figure 1 illustrates the 4CM granite bench and his UHV chamber installed in CARNAÚBA beamline.

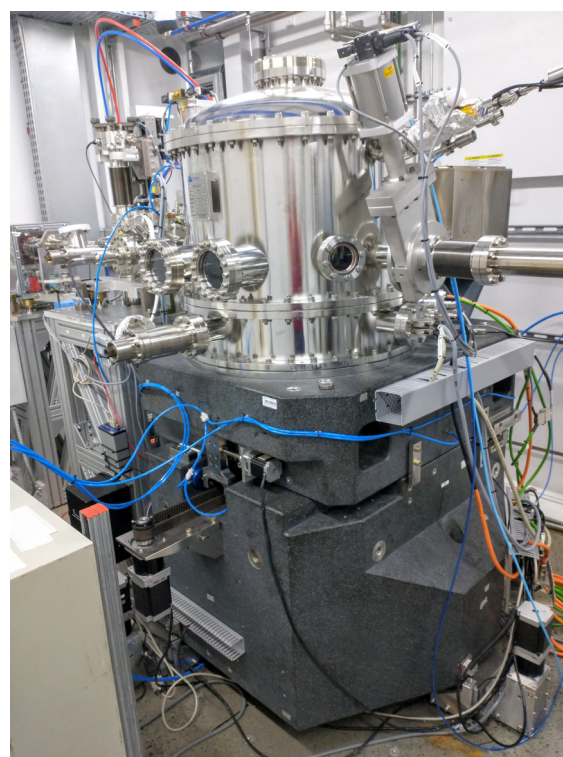


Figure 1: 4CM granite bench and UHV chamber.

Content from this work may be used under the terms of the CC BY 3.0 licence (© 2022). Any distribution of this work must maintain attribution to the author(s), title of the work, publisher, and DOI

### Motion Controller

The motion controller used in this system is the PBLV. The PWM amplifier is able to provide currents of 5 A continuous and 15 A of peak and has maximum switching frequency of 30 kHz. It is able to decode differential quadrature and BiSS-C encoders, necessary in this project, besides others types of protocols [5].

It was considered the use of the Epaq, but for limitations encountered in the available features, the PBLV was chosen. As the standard motion controller for medium and high complexity applications in Sirius's beamlines, PBLV makes coordinating and triggering with other systems more compatible. In compensation, it was challenging to maintain the same Epaq performance, due to his linear amplifiers.

### Crystals

The incoming pink beam is diffracted four times by two Si-111 channel-cut crystals, disposed in the configuration -++-. In this configuration, the crystals rotates in opposite directions, as seen in Fig. 2. In order to guarantee that the beam doesn't suffer any offset, is essential the channel-cut crystals have equal gap between his optical surfaces and the parallelism at each channel-cut.

From the Bragg's law, described in Eq. (1), we have the relation of the angle of diffraction (crystal angle  $\theta$ ) and wavelength ( $\lambda$ ) of the output beam, being the first diffraction order and given the distance of crystallographic planes  $d = 3.135\ 416\ 1\ \text{\AA}$  for Si-111.

Equation (2), that describes the photon energy ( $E$ ) from: Planck's constant ( $h$ ), speed of light ( $c$ ) and wavelength ( $\lambda$ ).

Substituing Eq. (1) in Eq. (2), we get the energy ( $E$ ) in function of diffraction angle ( $\theta$ ), as described in Eq. (3).

$$\lambda = 2d \sin(\theta) \tag{1}$$

$$E = \frac{hc}{\lambda} \tag{2}$$

$$E = f(\theta) = \frac{hc}{2d} \frac{1}{\sin(\theta)} \tag{3}$$

Each crystal are positioned by a direct-drive rotary stage, Aerotech APR200DR-155 (APR), indicated in Fig. 2 item d. It consists in permanent magnet synchronous motor (PMSM), Hall sensors and Renishaw's interpolated quadrature encoder system, with two readheads 180° spaced, each on with an angular resolution of 26.6 nrad [6].

### Mask

A mask is used to prevent reflections and spurious diffractions contaminates the output beam. It must be positioned based on the beam offset caused by the first pair of diffractions, which is function of the angle of the first channel-cut angle ( $\theta_1$ ) and the gap between the optics surfaces, described in the Eq. (4) and illustrated in Fig. 2.

$$Offset = 2 \cdot gap \cdot \cos(\theta_1) \tag{4}$$

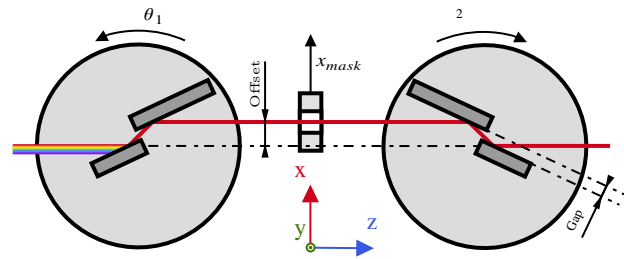


Figure 2: Representation of the crystals and mask. Indicating: the beam offset; the crystals gap; the adopted directions as positive for upstream crystal ( $\theta_1$ ), downstream crystal ( $\theta_2$ ) and mask; and the Sirius' coordinate system ( $x_{mask}$ )

A screw-driven linear stage, Aerotech MPS50SL-025 (MPS) moves the mask between both crystal, indicated in Fig. 3 item c. In the configuration present at this application encloses a DC brush servomotor with 14:1 gearbox, a screw with 1 mm/rev of pitch, a rotary encoder with 512 lines/rev; resulting a resolution 34.8 nm at the load [7]. As the encoder is situated at motor's axis, one of the precautions taken during metrology procedures was to ensure that there is no considerable backlash. MPS also carries a diagnostic device, being a photodiode in CATERETÊ and a gold plated part in CARNAÚBA, that generates electrons by photoelectric effect.

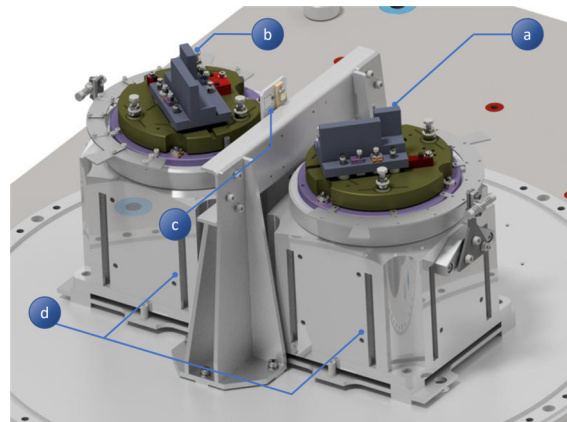


Figure 3: UHV components 3D model, namely: indicates upstream crystal; (b) indicates downstream crystal; (c) indicates the mask; (d) indicates the APR stages.

## GRANITE BENCH KINEMATICS

The UHV chamber position is set by the relative motion of the stacked granite blocks performed by both motorized air-bearings and levelers mechanisms. The coordinated motion of all actuators enhances the user experience since the embedded kinematics [8] moves the control point in relation to the laboratory reference frame and no hand calculations of actuators position is needed.

The 4CM bench has a customized control point feature, playing an important role during alignment since the user

has three options for setting the reference frame<sup>1</sup>: rotation axis of the upstream or downstream crystal, and the midpoint between them.

## DC BRUSH CONTROL

Having the DC brush a low rated current (0.16 A), was used the PBLV function PWM scale-factor, limiting the duty cycle [9] in 40 %, in order to avoid damage to the motor. A phase fuse was also included for redundancy.

The position control of the MPS stage have relatively more relaxed restrictions, due the usual small displacements and the size of the mask comparing to the beam size.

## PMSM CONTROL

### Phase Commutation

The phase commutation of the PMSM of the APR stage is made using the PBLV's algorithm, using the direct-quadrature-zero transform, common in field-oriented control (FOC).

As stage encoders are incremental, it is necessary to use Hall sensors for proper phase switching until the position is referenced by the home procedure; after this, having previously been characterized the rotor angle at position reference, the encoder is used as phase position feedback for higher resolution in commutation.

### Current Control

Each phase of the APS stage have as electrical nominal specifications of resistance of 4.4 Ω and inductance of 1.7 mH. Low values of inductance motors are commonly susceptible to induced noise due current ripple caused by PWM drivers, like the one used in the PBLV.

In order to mitigate this kind of problem, a switching frequency of 20 kHz it was used. Even so, that did not prevent undesirable oscillations in the position reading.

Tests were made adding series inducers in each phase, but no significant improvement was observed, not even any correlation with the resultant inductance value.

The best results were achieved using the voltage-mode and adjusting the gains of the PBLV current-loop<sup>2</sup> to behave as a "pass-through" [10]. As trade-off, there is no proper torque control, what is not critical for this system.

### Servo Control

The position and velocity control is made using the PBLV's standard servo-loop, which permits adjust digital filters, proportional-integrative-derivative (PID) and feed-forward gains.

Since the current-loop is not being closed for the APR stage, acting as a gain, the servo-loop was configured to be executed at the phase interruption, eliminating a full phase-cycle delay, what makes the servo-loop be executed at the

<sup>1</sup> The control point could be set anywhere changing the kinematics parameters. Those predefined points were chosen by the beamlines' staff

<sup>2</sup> Integrative gain have no effect for voltage-mode

same frequency of the phase algorithm, 20 kHz, improving even more the stability of the system.

On other hand, this configuration makes that encoder conversion tables are not processed, because they runs at the servo interruption, so the position and velocity feedback is processed at the same manner of the phase position [11]. The result of this is the loss of capacity of make average between the signals from both encoders present at the stage, a technique used to minimize errors from encoder interpolation and scale imperfections [12].

The stability of each APR stage was evaluating the position error, at a 20 kHz rate, for angles between 0° and 18° and the resulting cumulative amplitude spectrum (CAS) is presented in the Fig. 4. The values to each angle, integrating from 1 Hz to 2500 Hz, is as presented in the Table 1. Figure 4 make it clear that there are some well-defined frequencies that impact the stability of the system.

Table 1: Position Error CAS (1 Hz-2500 Hz)

Angle	Upstream Position Error	Downstream Position Error
0°	24.6 nrad	39.2 nrad
3°	24.6 nrad	33.3 nrad
6°	25.1 nrad	34.6 nrad
9°	20.2 nrad	34.6 nrad
12°	22.2 nrad	34.8 nrad
15°	21.6 nrad	39.1 nrad
18°	19.0 nrad	33.9 nrad

As a disclaimer, this test does not cover the whole stage position range, due to mechanical problems.

## CRYSTALS COORDINATION

One of the most important requirements, besides the position stability, is the coordination between the crystals, in other words, how accurate is energy selected by the two channel-cut crystals. The tolerance is defined based in the crystal energy resolution and diffraction angle. Using the worst-case, the coordination error should be maintained below 1 μrad.

### Epaq Coordination Modes

During the analysis of coordination using the Epaq controller, it was noticed that the suggested operation mode for this kind of operation, denominated electronic gearing, results in errors far beyond the acceptable limit for this application. This error occurs also in the difference of setpoints, indicating that there is a lag between the commands for both stages. The tests are at constant velocity of 1 °/s and results in coordination errors of approximately 210 μrad.

Another studied method was the gantry mode, in which satisfactory results were obtained around 1 μrad. However, this kind of operation sets one of the stages as the follower, disabling any input command from the user, that is necessary during the monochromator calibration. To toggle this mode,

Content from this work may be used under the terms of the CC BY 3.0 licence (© 2022). Any distribution of this work must maintain attribution to the author(s), title of the work, publisher, and DOI

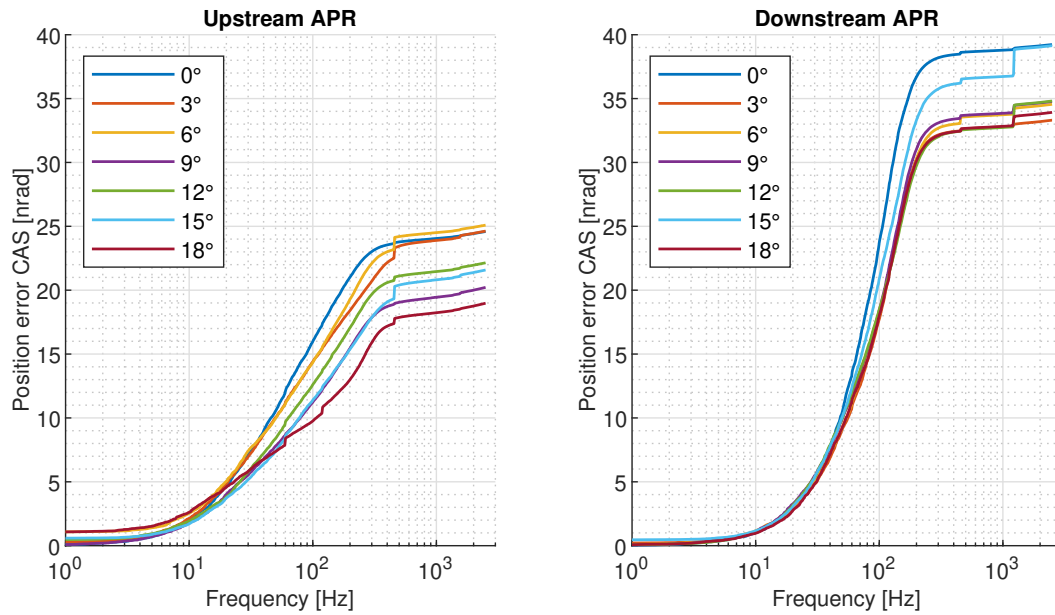


Figure 4: Cumulative amplitude spectrum in position error at each angle.

it is necessary to reset completely the Epaq, making loose the position reference. Also, with gantry mode enabled, the limits of the follower stage are not respected, being unwanted for system integrity.

Figure 5 compares this two modes, together with the coordination error when commanding both stage at the same command line, to the same position, namely uncoupled.

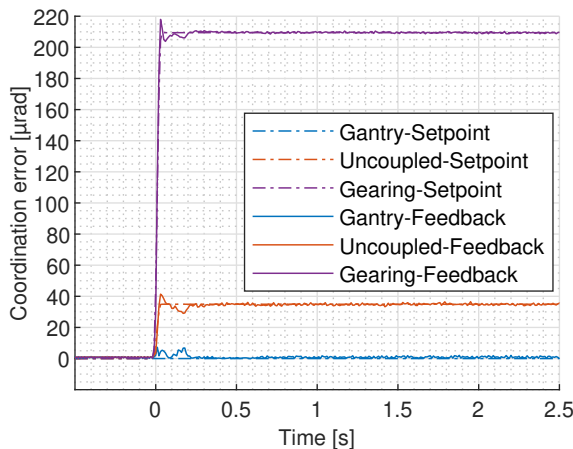


Figure 5: Ensemble Epaq MR coordination modes.

### PBLV Coordination

In was used the native kinematics scripts for the transform energy (user input) in angle (in encoder counts units), also implements the coordinated movement between the crystals, being available an offset in the angle of each crystal for the monochromator energy calibration purposes.

Evaluating the coordination error at the same velocity of the tests with Epaq, 1 %/s, we can observe that, neglecting

pike of 20 μrad occurred in acceleration period, the error is well behaved, remaining below 1 μrad, as seen in Fig. 6.

Possibly adding proper feedforward gains attenuate the error during the acceleration. Furthermore, it possible to use the PBLV feature of gantry cross-couple, causing the error of one of the stages to be taken into account in the servo-loop of the other.

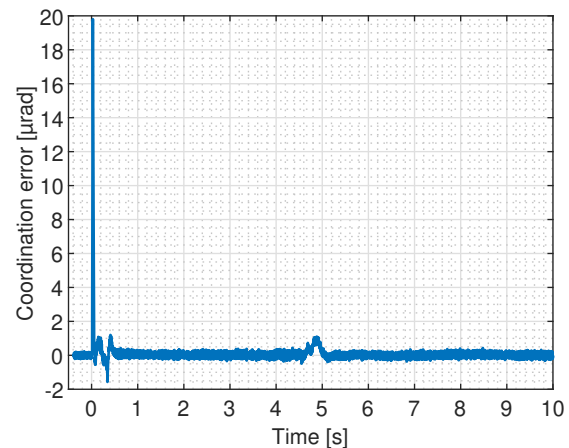


Figure 6: Power Brick LV coordination error.

## CONCLUSION

The results of implementation of control for 4CM had satisfactory results, but there still scope for improvements- e.g. adjustment of feedforward and gantry cross-couple gains, coordination with undulator and investigation of noise sources.

This work also put to the test the capabilities of the PBLV controller, which is of great value for new complex projects to be developed for Sirius.

## ACKNOWLEDGEMENTS

The authors would like to gratefully acknowledge the funding by the Brazilian Ministry of Science, Technology, Innovation and the contribution of the LNLS team.

## REFERENCES

- [1] Sirius Project, <https://www.lnls.cnpem.br/sirius-en/>.
- [2] Tolentino, H.C.N., et al., “X-ray microscopy developments at Sirius-LNLS: first commissioning experiments at the Carnauba beamline”, in *Proc. SPIE 11839, X-Ray Nanoimaging: Instruments and Methods V*, 2021, p. 1183904.
- [3] F. Meneau *et al.*, “Cateretê, the Coherent Scattering Beamline at Sirius, 4th Generation Brazilian Synchrotron Facility”, in *Coherence at ESRF-EBS, Grenoble, France*, 2019.
- [4] R. Geraldès *et al.*, “Granite benches for Sirius X-ray Optical Systems”, in *Mechanical Engineering Design of Synchrotron Radiation Equipment and Instrumentation*, Paris, France, 2018. doi:10.18429/JACoWMEDSI2018-THPH12
- [5] *Power Brick LV ARM User Manual*, Delta Tau Data Systems, Inc., Los Angeles, CA, USA, Dec. 2020, pp. 14-20, <https://assets.omron.com/m/661730249d3863b4/original/Power-Brick-LV-ARM-User-Manual.pdf>
- [6] *APR Hardware Manual*, Aerotech Inc., PA, Pittsburgh, United States, Jun. 2018; <https://www.aerotech.com/wp-content/uploads/2021/01/APR.pdf>
- [7] *MPS50SL Hardware Manual*, Aerotech Inc., PA, Pittsburgh, United States, Jan. 2020; <https://www.aerotech.com/wp-content/uploads/2021/01/MPS50SL.pdf>
- [8] G. N. Kontogiorgos, A. Y. Horita, L. Martins dos Santos, M. A. L. Moraes, and L. F. Segalla, “The Mirror System Benches Kinematics Development for Sirius/LNLS”, presented at ICALEPCS’21, Shanghai, China, Oct. 2021, paper TUPV001, this conference.
- [9] G. N. Kontogiorgos, C. S. B. N. Roque, and M. A. L. Moraes, “Motion Control Improvements for Kirkpatrick-Baez Mirror System for Sirius/LNLS EMA Beamline”, presented at ICALEPCS’21, Shanghai, China, Oct. 2021, paper TUPV002, this conference
- [10] *Power PMAC User’s Manual*, Delta Tau Data Systems, Inc., Los Angeles, CA, USA, Jan. 2021, pp. 275-276; <https://assets.omron.com/m/2c1a63d391d6bfa3/original/Power-PMAC-Users-Manual.pdf>
- [11] *Power PMAC User’s Manual*, Delta Tau Data Systems, Inc., Los Angeles, CA, USA, Jan. 2021, pp. 302-303; <https://assets.omron.com/m/2c1a63d391d6bfa3/original/Power-PMAC-Users-Manual.pdf>
- [12] Hayama, S., Duller, G., Sutter, J. P., Amboage, M., Boada, R., Freeman, A., Keenan, L., Nutter, B., Cahill, L., Leicester, P., Kemp, B., Rubies, N., and Diaz-Moreno, “The scanning four-bounce monochromator for beamline I20 at the Diamond Light Source”, *Journal of synchrotron radiation*, vol. 25, no. 5, pp. 1556–1564. doi:10.1107/S1600577518008974